

Nonlinear Model Validation using Multiple Experiments

Wayne J. Dunstan
Automation & Controls Laboratory
GE Global Research
Niskayuna, NY 12309, USA
dunstan@research.ge.com

Robert R. Bitmead*
Dept of Mechanical & Aerospace Engineering
University of California San Diego
La Jolla, CA 92093-0411, USA.
rbitmead@ucsd.edu

Abstract—Model validation is the formulation of an experiment to test the predictive power of a candidate model. This paper considers an atypical method for combining multiple experiments, which arises due to our choice of measure. We explore a framework for combining multiple experiment information using bifurcation theory. We follow the approach of successive deduction, hypothesis formulation and falsification testing in an attempt to invalidate a given model. The example used to illustrate the method is the practical problem of combustion instability modelling.

I. INTRODUCTION

Model validation, or more aptly corroboration, is the formulation of an experiment to test the predictive power of a candidate model. The objective is not to create an experiment which supports the model, but in fact one which attempts to falsify an *a priori* model hypothesis.

This idea of experiment conjecture and hypothesis refutation was proposed by K. Popper [Pop59]. Popper described the set of methodological rules called *Falsificationism*. Instead of a model structure being discovered and verified by way of inductive generalizations identified from data, Popper argued that modelling knowledge advances instead by deductive falsification. Experiment and observation test hypotheses, not produce them.

In our work we seek a nonlinear model suitable for control design. This requires a parsimonious model which captures the system behavior over different operating points. Two of the challenges facing us are,

- 1) how to alter the model structure systematically and parsimoniously, and,
- 2) how to use multiple experiment data, possibly at different operating points, in the model validation task.

The first challenge to which we have already alluded, is connected to Popper's concepts of falsification. However formal tools to tackle the second challenge, are not immediately apparent in the nonlinear context considered here.

In prediction-error identification methods, a standard validation technique involves conducting independent experiments at the same operating point, and comparing this data to the predicted outputs from the model. Validation tools for this type of problem are readily available [Lju99], [SS89].

The example considered here however, uses a spectral measure of fit and multiple sets of data at different operating

points. These conditions do not lend themselves to the standard multiple experiment fixed operating point validation techniques, because the signal spectra do not change significantly. We shall have to seek other tests. The central issue though still remains to exploit and stress the predictive power of the model.

In our example of a limit-cycling combustion instability we are faced with multiple narrow band experiments, each of which is not particularly informative. Combined however, they contain significant information about the system behavior. We shall attempt to modify a given model parsimoniously, using techniques of hypothesis falsification and nonlinear tools for combining multiple experiment data.

II. EXPERIMENTAL DATA

The system being modelled is a thermo-acoustic combustion instability which can occur in the combustion chamber of many propulsion and power generation engines, e.g. industrial gas turbines and jet engines. This instability is believed to stem from the positive feedback coupling between linear acoustics and the nonlinear heat release from the combustion process [PP98].

Six experiments without external excitation signals were conducted in a combustion chamber at different fuel-to-air ratios, ϕ , where the combustion instability was present. The signals measured were the downstream pressure fluctuations, \bar{p}_k , and heat release rate, \bar{q}_k . The spectrogram (time-frequency-magnitude) plots for \bar{p}_k and \bar{q}_k for all six experiments are shown in Figures 1 and 2 respectively. The following preliminary observations can be made:

- The \bar{p}_k and \bar{q}_k data are dominated by a strong sinusoid at $\sim 210\text{Hz}$ (ω_1), a weaker broader signal at $\sim 740\text{Hz}$ (ω_2), and harmonics of ω_1 .
- The fundamental, ω_1 , decreases in frequency for decreasing values of ϕ .
- The \bar{q}_k data do not display the high frequency components present in \bar{p}_k , due to the heat release rate sensor exhibiting a low pass filtering effect.

III. DEDUCTIVE MODEL STRUCTURE 1

The candidate parametrized model is shown in Figure 3. It is parametrized by two parallel oscillators (ω , ξ , N , M), two differentiators, a time delay (τ), and static memoryless nonlinearity ($\psi[\cdot]$) in feedback. The Anti-Aliasing Filters (AAF) and Low Pass Filter (LPF) effect have been added

*Research supported by USA National Science Foundation Grant ECS-0070146 and DARPA Grant N00014-00-1-0799

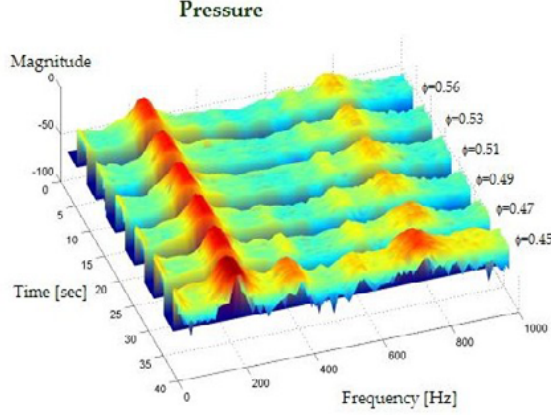


Fig. 1. Multiple experiment pressure signals.

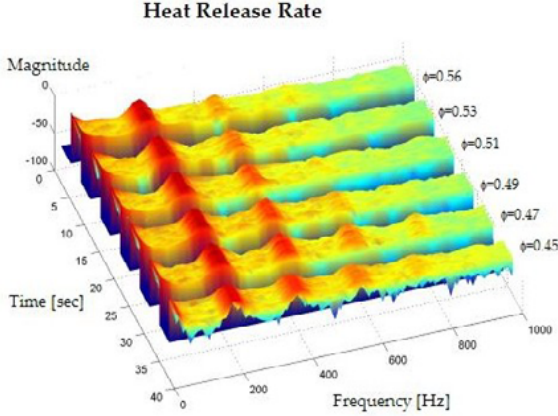


Fig. 2. Multiple experiment heat release rate signals.

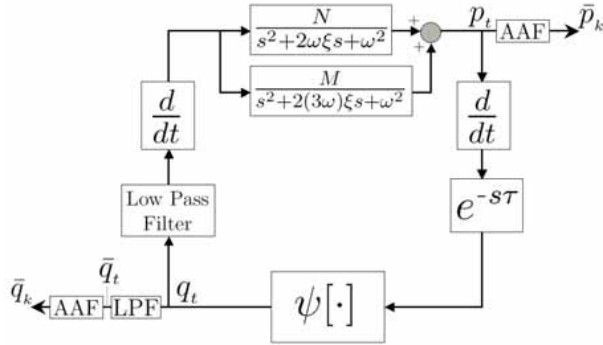


Fig. 3. Candidate Model.

to capture how the measured signals might differ from the signals in the loop.

A. Deductions

The following physical deductive reasoning was used in creating the model of Figure 3.

- The linear acoustics (M, N, ω, ξ) of the combustion

chamber are primarily a function of the chamber geometry and as such are expected not to change with ϕ .

- The delay, τ , is a bulk delay composed primarily of the propagation time between the injector and the flame front. This is believed to be constant.
- The heat release function, $\psi[\cdot]$, should resemble a negative slope saturation. The slope of the heat release function, $\psi'[\cdot]$, represents the sensitivity of the heat release function to pressure variations. Combustion theory argues that as ϕ decreases, this sensitivity will increase, corresponding to increased pressure variations.
- The phase of the LPF should have little effect on the phase of \bar{q}_k component at ω_1 if as we suspect the LPF transition band is above 500Hz.

B. Fitting

The fitting of the model in Figure 3 has been considered in detail in [MJC⁺98], [SBD01], [DBS01]. Because the ω_2 oscillation does not appear in the \bar{q}_k data these fitting techniques have relied primarily on the following two estimates from the data.

- $\tilde{\omega}_1$ Estimated frequency of the fundamental ω_1
- $\tilde{\Delta}_{\bar{p}\bar{q}}(\tilde{\omega}_1)$ Estimated phase shift from \bar{p}_k to \bar{q}_k at $\tilde{\omega}_1$

Table I summarizes the estimates over the six experiments. The works of [MJC⁺98], [SBD01], [DBS01] have used a

TABLE I
SUMMARY OF ESTIMATED QUANTITIES.

Exp. No.	ϕ_n	$\tilde{\omega}_1$ [Hz]	$\tilde{\Delta}_{\bar{p}\bar{q}}(\tilde{\omega}_1)$ [DEG]
1	0.56	211	6
2	0.53	209	10
3	0.51	206	14
4	0.49	203	19
5	0.47	199	23
6	0.45	180	43

reductionist type approach to fitting due to the paucity of spectral information. By reductionist, we mean fitting small sections of the loop individually and then combining these results together to produce a complete model fit.

For example the delay is identified by considering the phase change between \bar{p}_k and \bar{q}_k and subtracting off the static phase elements i.e. the differentiator and the nonlinearity. The nonlinearity is identified by reconstructing its input signal by mapping each periodic component in \bar{p}_k to reproduce the input to $\psi[\cdot]$. With this signal and \bar{q}_k , we plot the nonlinearity. The oscillator parameters are fitted using the succession of permissible loop phase values at the fundamental oscillating frequency over the range of six experiments.

Combining these estimates we are able to fit all of the model parameters [SBD01], [DBS01].

C. Hypothesis

Based upon these deductions and fitting results the following hypothesis is proposed:

Hypothesis 1: The behavior of the model parameters as the fuel-to-air ratio ϕ decreases is as follows:

Par. No.	Parameter	Behavior as $\phi \downarrow$
1	M	fixed
2	N	fixed
3	ω	fixed
4	ξ	fixed
5	τ	fixed
6	$\psi'[\cdot]$	increases
7	Δ_{LPF}	fixed

This seemingly-plausible and physically reasonable hypothesis, if true, would offer some insight into the controller design for this model. In the methodology of Popper [Pop59], we now attempt to reject this hypothesis.

IV. TESTING HYPOTHESIS 1

Our aim now is to create systematically falsification tests to reject Hypothesis 1. This is the method of *trial and elimination of error by criticism* [Pop94].

Falsification tests are designed to carefully test the model validity boundaries, defined by a hypothesis, in such a way that they expose a specific deficiency in the current model.

A. Falsification Test 1

The first test is to check the multi-experiment behavior of τ . If the estimated delay in the reductionist model is constant across experiments, then this supports Hypothesis 1. If the delay is not constant across experiments, then Hypothesis 1 is rejected.

The delay, τ , is identified from the equation for $\tilde{\Delta}_{\bar{p}\bar{q}}(\omega_1)$,

$$\Delta_{\bar{p}\bar{q}}(\omega_1) = \Delta_{\frac{d}{dt}} - \Delta_{\tau}(\omega_1) + \Delta_{\psi[\cdot]} + \Delta_{LPF}, \quad (1)$$

where Δ is used to denote phase change. Considering each of the terms on the RHS of (1):

- The differentiator and nonlinearity contribute $\frac{\pi}{2}^c$ and π^c respectively.
- The phase due to the delay at ω_1 is equal to $\omega_1 \cdot \tau$
- The lowpass filter (LPF) affecting \bar{q}_k is assumed to roll off outside the bandwidth of the ω_1 , implying

$$\Delta_{LPF} = c \quad \forall \omega_1 < 2\pi \cdot 500$$

where c is a constant.

Substituting this information into (1) gives,

$$\begin{aligned} \Delta_{\bar{p}\bar{q}}(\omega_1) &= -\omega_1 \cdot \tau + \left(\frac{3\pi}{2} + c\right) \\ &= -\omega_1 \cdot \tau + c' \end{aligned} \quad (2)$$

where c' is a constant. Plotting $\tilde{\omega}_t$ vs $\tilde{\Delta}_{\bar{p}\bar{q}}(\omega_1)$ reveals a linear relationship, where according to (2) $\tau = 3.52\text{msec}$, constant for all ϕ .

This supports Hypothesis 1, and so we proceed to another falsification test to stress the model's capabilities further.

B. Falsification Test 2

The second test is to check the multi-experiment spectral simulation capabilities of the mode. It is not reductionist like the first test – it examines properties of the entire nonlinear closed loop.

The data contains a steadily decreasing ω_1 for decreasing fuel-to-air ratio, ϕ , and the model should capture this. If it does not then Hypothesis 2 is rejected.

We explore the existence of sustained periodic solutions using bifurcation theory [GH83]. The bifurcation diagram for the constant-delay differential equation depicted in Figure 3, using the constant identified parameter values and the ϕ -varying $\psi'[\cdot]$ from [DBS01], is shown in Figure 4. The

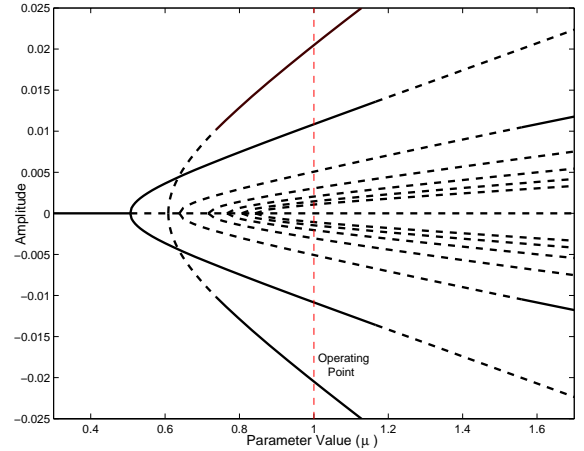


Fig. 4. Bifurcation diagram.

horizontal axis depicts the gain parameter μ , which increases with $\psi'[\cdot]$, and the vertical axis shows the amplitude of stationary points and orbits of the system. Each branch of the bifurcation diagram indicates the stability (solid line) or instability (dotted line) of the associated orbit at the particular parameter value.

The ϕ_1 operating point is shown by the thin vertical dashed line at $\mu = 1.0$. The bifurcation diagram predicts that the measurements should contain a large amplitude 211Hz stable orbit and a smaller amplitude 740Hz stable orbit - exactly as is seen in the data.

A simulation of the identified model at ϕ_1 produces a spectrum almost identical to the spectrum of the ϕ_1 data. The simulated model is driven by a perturbation component to allow continual transitions between the two stable orbits, as described by [DBS01].

In the bifurcation analysis, μ adjusts the loop gain, and hence can be written as a function of nonlinearity gain,

$\psi'[\cdot]$. Hypothesis 1 says that as ϕ decreases, $\psi'[\cdot]$ increases. Hence there exists a mapping which describes increasing μ for decreasing ϕ .

The model predicts constant ω_1 and ω_2 for varying ϕ in the range $\phi = 0.56 \rightarrow 0.46$ ($\mu = 1.0 \rightarrow 1.6$). This disagrees with the information of Table I, which shows increasing ω_1 for decreasing ϕ . Therefore the test fails and we reject Hypothesis 1. This invalidates Model 1 because it fails to explain the data.

V. DEDUCTIVE MODEL 2

We now seek a parsimonious way to alter Model 1 that is a deductive step in moving to a new model. The aim is to create a new hypothesis which (at least) passes the previous test with the minimum amount of additional complexity.

A. Deductions

In deciding which part of our physical reasoning to amend we consider each of the model components as before.

- The linear acoustics (M, N, ω, ξ) could change with gas density changes, however initially at least, this is believed to be a second order effect. Therefore we leave this unchanged.
- The delay τ should be tightly coupled to the fluctuations in the flame front. As ϕ is lowered, the instability grows, and the mean flame front increases in length. This would increase the propagation time between the injector and the flame front, thereby increasing τ . Therefore we might postulate a variable τ .
- The heat release function, $\psi[\cdot]$ we leave unaltered from before.
- The phase of the LPF may have a transition band around ω_1 . This may interact with the phase introduced by changing τ .

B. Fitting

Incorporating a multi-experiment varying- τ into the model requires the re-assessment of the reductionist identification procedure. We now have to account for the variability in τ and the phase of the LPF, using the same estimates from Table I.

Consider again the phase calculation in (1). The description of the RHS is as before except,

- the delay is now a function of ϕ , so the phase change due to the delay at ω_1 is equal to $\omega_1 \cdot \tau(\phi)$, and
- the LPF affecting \bar{q}_k may have a transition band which includes ω_1 , implying

$$\Delta_{LPF} = f(\omega_1)$$

Substituting this information into (1) gives,

$$\Delta_{\bar{p}\bar{q}}(\omega_1) = -\omega_1 \cdot \tau(\phi) + f(\omega_1) + \frac{3\pi}{2} \quad (3)$$

Plotting $\tilde{\omega}_1$ versus $\tilde{\Delta}_{\bar{p}\bar{q}}(\omega_1)$ for ϕ_1 to ϕ_6 produces a constant slope plot [SBD01].

With fixed acoustics, we may appeal to describing function analysis to predict the required delay, τ , for a given oscillation frequency. This corresponds to rotating the Nyquist diagram of the fixed linear part of the model. Using the $\tilde{\omega}_1$ values from Table I we predict the corresponding delays, $\hat{\tau}$, for each experiment shown in Table II. The next column

TABLE II
PHASE CALCULATIONS.

Exp. No.	$\hat{\tau}$ [ms]	$\hat{\Delta}_{pq}(\tilde{\omega}_1)$ [degrees]	$\hat{\Delta}_{\bar{p}\bar{q}}(\tilde{\omega}_1)$ [degrees]	$\hat{\Delta}_{LPF}$ [degrees]
1	3.52	3	6	3
2	3.59	0	10	10
3	3.69	-4	14	18
4	3.80	-8	19	27
5	3.95	-13	23	36
6	4.75	-38	43	81

across shows the phase between p_t and q_t (i.e. inside the loop) introduced by these predicted delays at the estimated frequencies, given by,

$$\hat{\Delta}_{pq}(\tilde{\omega}_1) = -\tilde{\omega}_1 \cdot \hat{\tau} + \frac{3\pi}{2}.$$

The last column is predicted phase attributed to the LPF, $\hat{\Delta}_{LPF}$, given by,

$$\hat{\Delta}_{LPF} = \tilde{\Delta}_{\bar{p}\bar{q}}(\tilde{\omega}_1) - \hat{\Delta}_{pq}(\tilde{\omega}_1).$$

The plot of this LPF phase response is shown in Fig 5. Notice

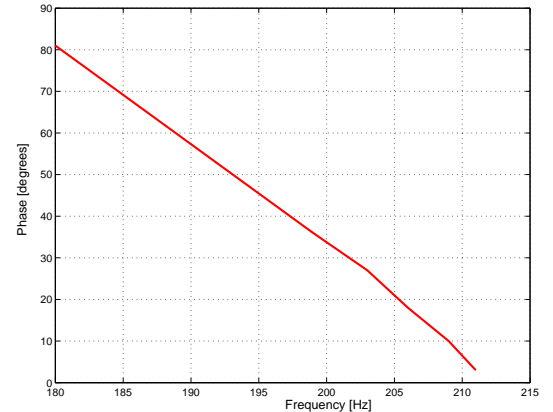


Fig. 5. Predicted phase response for the LPF over the range ϕ_1 to ϕ_6 .

the shape of this plot is an acceptable LPF response, hence the fitting is able to explain the observed estimates using the modified deductions.

C. Hypothesis

Based upon the new deductions and the subsequent fitting, the next hypothesis is proposed:

Hypothesis 2: The behavior of the model parameters as the fuel-to-air ratio ϕ decreases is as follows:

Par. No.	Parameter	Behavior as $\phi \downarrow$
1	M	fixed
2	N	fixed
3	ω	fixed
4	ξ	fixed
5	τ	increases
6	$\psi'[\cdot]$	increases
7	Δ_{LPF}	increases

VI. TESTING HYPOTHESIS 2

We now apply the same falsification test that rejected Hypothesis 1, in an attempt to reject Hypothesis 2.

A. Falsification Test 2 Applied to the Second Model

The second falsification test checks the multi-experiment spectral simulation capabilities of the model. We do this again using a new bifurcation diagram which incorporates a parameter dependent delay, i.e. $\tau(\phi)$, across the ϕ range of interest. We only change τ across the ϕ range of interest as we have no knowledge of how τ behaves outside this range. Indeed we would suspect it to be constant for high ϕ values, where the flame front is steady.

The bifurcation diagram again predicts a large amplitude 211Hz stable orbit and a smaller amplitude 740Hz stable orbit as before, however now we are interested in how the period of ω_1 and ω_2 changes for changing μ - i.e. the multi-experiment behavior.

Figure 6 shows how the periods of ω_1 and ω_2 change for changes in μ , over the corresponding ϕ range of interest. The

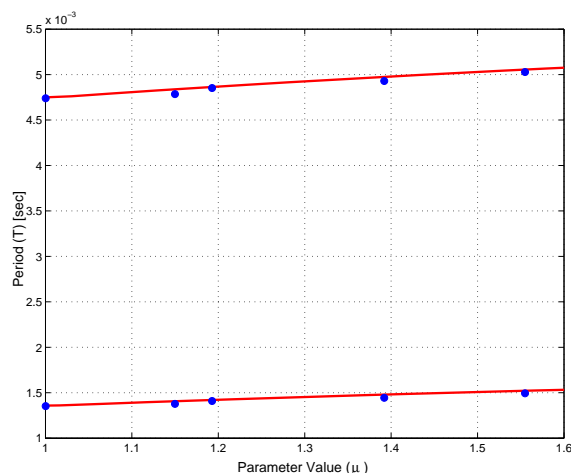


Fig. 6. Predicted changes in period for ω_1 (upper) and ω_2 (lower) as loop gain changes.

large dots denote where the $\tilde{\omega}_1$, $\tilde{\omega}_2$ and describing function analysis predicted oscillations would occur. Notice that the

model predicts decrease in ω_1 and ω_2 (increase in periods) with decreasing ϕ (increasing μ).

Therefore Hypothesis 2 is not rejected. We note that we have survived the new validation test at the expense of a more complicated model. Given the six data points we could devote even more effort to improving the fit by modifying $\tau(\phi)$. We believe our efforts are better spent developing a more rigorous falsification test for this second model.

VII. CONCLUSION

This paper has discussed a technique for nonlinear model validation using multiple experiments. Because the measure of fit criterion was not a prediction error method, but in fact a spectral method, we have had to employ other tools for combining multiple experiment data. This technique has been demonstrated to improve the model consistency using a parsimonious improvement strategy. The iterated model captures more of the important underlying system dynamical properties, at the expense of a slight increase in complexity. Overall this is viewed as a positive step towards a model more suitable for control design.

VIII. REFERENCES

- [DBS01] W.J. Dunstan, R.R. Bitmead, and S.M. Savaresi. Fitting nonlinear low-order models for combustion instability control. *Control Engineering Practice*, 9:1301–1317, 2001.
- [GH83] J. Guckenheimer and P. Holmes. *Nonlinear Oscillations, Dynamical Systems and Bifurcations of Vector Fields*. Springer-Verlag, 1983.
- [Lju99] L. Ljung. *System Identification: theory for the user*. Prentice-Hall, Englewood Cliffs, 2nd edition, 1999.
- [MJC⁺98] R.M. Murray, C.A. Jacobson, R. Casas, A.I. Khibnik, C.R. Johnson Jr, R.R. Bitmead, A.A. Peracchio, and W.M. Proscia. System identification for limit cycling systems: a case study for combustion instabilities. *American Control Conference, Philadelphia, USA*, pages 2004–2008, 1998.
- [Pop59] K. Popper. *The Logic of Scientific Discovery*, volume 1st. Hutchinson & Co. LTD, 178-202 Great Portland Street, London W1, fourth edition, 1959.
- [Pop94] K. Popper. *The Myth of the Framework*, volume 1st. Routledge, 29 West 35th Street, New York, NY 10001, 1994.
- [PP98] A.A. Peracchio and W.M. Proscia. Nonlinear heat-release/acoustic model for thermoacoustic instability in lean premixed combustors. *43rd ASME/IGTI Turbo Expo, Stockholm, Sweden*, 1998.

- [SBD01] S.M. Savaresi, R.R. Bitmead, and W.J. Dunstan. Nonlinear system identification using closed loop data with no external excitation: The case of a lean combustion chamber. *International Journal of Control*, 74:1796–1806, 2001.
- [SS89] T. Soderstrom and P. Stoica. *System Identification*. Prentice-Hall International (UK), 1989.